Corrosion Science xxx (2015) xxx–xxx

Contents lists available at ScienceDirect

Corrosion Science

journal homepage: www.elsevier.com/locate/corsci

Geobacter sulfurreducens: An iron reducing bacterium that can protect carbon steel against corrosion?

Claudia Cote *, Omar Rosas, Régine Basseguy *

Université de Toulouse, INPT, UPS, Laboratoire de Génie Chimique, BP 84234, 4 allée Emile Monso, F-31432 Toulouse cedex 4, France
CNRS, Laboratoire de Génie Chimique, F-31432 Toulouse, France

ARTICLE INFO

Article history:
Received 9 January 2015
Accepted 27 January 2015
Available online xxxx

Keywords:
A. Mild steel
B. EIS
C. Microbiological corrosion

ABSTRACT

The effect of *Geobacter sulfurreducens* on the electrochemical behaviour of carbon steel in anaerobic phosphate solution is studied here. In natural environments, *G. sulfurreducens* is able to reduce Fe(III) to Fe(II) during the oxidation of acetate. High availability of Fe(II) promoted the formation of an iron (II) phosphate layer on the steel. It is assumed that this phosphate layer, formed only when bacteria were present, is responsible for maintaining the corrosion potential stable even after intrusion of air. In contrast, the corrosion potential in the abiotic experiments suffered an increase of 450 mV after few hours of exposure to air.

1. Introduction

Microbial development occurs in almost all environments through biofilm formation and may be responsible for microbiologically-influenced corrosion (MIC), also known as microbial corrosion or biocorrosion, which can be defined as the enhancement or acceleration of corrosion by the presence of bacteria [1]. However, many authors have questioned the harmfulness of biofilms on metal surfaces and even argued that some of them may reduce corrosion rates by various mechanisms [2–5]. One of these mechanisms is a surface reaction leading to the formation of a corrosion-inhibiting layer of phosphate such as the iron phosphate named vivianite.

Vivianite is an iron (II) phosphate, $Fe_3(PO_4)_2{\cdot}8H_2O$, which may be used as a corrosion inhibiting agent of iron because of its low solubility: it forms a film of poorly soluble and non-oxidising corrosion product on the metal surface [4–7]. Corrosion inhibition is the slowing down of the corrosion reaction usually performed by substances (corrosion inhibitors) which, when added to an environment in small amounts, decrease the rate of attack by this environment on a metal [8]. A protection method against corrosion used by some industries is acid phosphating with phosphates of zinc, iron or manganese, which leads to vivianite production [4]. This procedure is carried out at temperatures of up to 95 °C and pH values between 2 and 3.5.

One of the most studied mechanisms of corrosion inhibition promoted by microorganisms, or microbially influenced corrosion inhibition (MICI), is corrosion control using beneficial biofilms [7–10]. These benefits can be linked either to physical characteristics of the biofilm or to biochemical characteristics involving metabolites. A biofilm is a highly organised bacterial community with cells entrapped in a matrix of extracellular polymer substances (EPS). On the one hand, the bacteria may form a persistent film adhering to the metal/solution interface and reducing the corrosion rate by forming a transport barrier, which may prevent the penetration of corrosive agents (such as oxygen, and chloride), decreasing their contact with the metal surface and thus reducing corrosion [7,8]. However, some studies have shown that this protection is not effective and that biofilms could instead promote corrosion by the formation of a non-uniform patch which, in the presence of aerobic respiration, results in the formation of a differential aeration cell, thus accelerating the corrosion rate [7,11]. On the other hand, corrosion inhibition is sometimes explained by the biochemical characteristics of the microorganisms themselves and/or their enzymes. For instance, a vivianite deposit was observed on mild steel electrodes placed in a galvanic cell in presence of hydrogenase from *Clostridium acetobutylicum* (an iron reducing bacterium – IRB) [12,13]. The consequence of this catalysed deposit was a delay in pitting corrosion or a reduced corrosion rate. Other authors [9,10,14,15], have claimed that different species of bacteria (most of them belonging to the IRB-group) induce a reduction of corrosion rates, the prevention of pitting

* Corresponding authors at: CNRS, Laboratoire de Génie Chimique, F-31432 Toulouse, France. Tel.: +33 5 34 32 36 17; fax: +33 5 34 32 27 00.
E-mail addresses: ccote@jouy.inra.fr (C. Cote), regine.basseguy@ensiacet.fr (R. Basseguy).

http://dx.doi.org/10.1016/j.corsci.2015.01.044
0010-938X/

corrosion and a reduction of both cathodic and anodic reaction rates for materials such as stainless steel [16], mild steel and aluminium brass [9,10]. Little et al. [16] and Eashwar et al. [17] have claimed that corrosion inhibition on stainless steel is due to a mechanism in which siderophores (iron chelators) produced by microorganisms within biofilms at neutral pH act as inhibitors and enhance the passivity of stainless steel by reducing the passivation current (i_p). Other mechanisms most frequently cited for MICI are resumed by Little and Ray [18] in a critical review. These mechanisms are: formation of a diffusion barrier to corrosion products that stifle metal dissolution, consumption of oxygen by respiring aerobic microorganisms within the biofilm causing a diminution of that reactant at the metal surface, production of metabolic products that act as corrosion inhibitors (e.g. siderophores, vivianite), production of specific antibiotics that prevent proliferation of corrosion-causing organisms (e.g., sulphate-reducing bacteria (SRB)), formation of passive layers that are due to the presence of microorganisms [18], reduction of ferric ions to ferrous ions (in presence of IRB) and increase consumption of oxygen [15,19]. Moreover, Herrera and Videla [20] claim that the introduction of IRB in industrial water systems that contain SRB and other corrosion-inducing bacteria causes not only the exfoliation of corrosion products but also the protection of the metal surfaces from further corrosion. In general, the main mechanisms of corrosion inhibition by bacteria are linked to a marked modification of the environmental conditions at the metal/solution interface by biological activity [20].

Moreover, IRB have been reported to biologically produce vivianite at laboratory scale under aerobic conditions with a few bacterial strains such as *Pseudomonas* sp. [2] and *Rhodococcus* sp., using a metal coupon and 20 mM of phosphate buffer [4,5,21]. Islam et al. [22] reported vivianite formation under anaerobic conditions by *Geobacter sulfurreducens* using soluble Fe (III) (iron citrate) as electron acceptor. When the organism was grown using insoluble crystalline Fe (III) and oxy-hydroxide as electron acceptor, Fe (III) reduction resulted in the formation of magnetite instead of vivianite. These same results were also observed by Lovley and Phillips [23].

G. sulfurreducens is a dissimilatory IRB thanks to its electron exchange capabilities with solid substrate [24]. However, its role in corrosion is still uncertain. Recent studies with *G. sulfurreducens* have shown that these bacteria can exert two different effects on 304L stainless steel: just after inoculation, G. *sulfurreducens* cells create a cathodic reaction on the material, which leads to a fast increase in its open circuit potential (OCP), heightening the corrosion risk. In contrast, after a few days, well established biofilms shift the pitting potential towards positive values, which may be interpreted as a protective effect [3]. This research concluded that *G. sulfurreducens* played a role in the corrosion behaviour of 304L, which depends on medium composition. In the absence of acetate (lack of electron donor), *G. sulfurreducens* biofilms promote the propagation of pitting whereas, in the absence of fumarate (lack of electron acceptor), *G. sulfurreducens* cells were able to delay pit occurrence, thus protecting the metal.

The controversy about enhancement of corrosion and/or protection against corrosion promoted by microorganisms is still unresolved regarding this bacterial group. According to some reports, IRB are able to induce protection of carbon steel [3,16,20] while others suggest a considerable increase of corrosion through the reduction and removal of passive films of ferric compounds on the metal surface [3,19,20].

On the other hand, iron reducers can have a major effect on the availability of iron ions through the solubilisation of insoluble iron compounds and the resulting formation of biominerals [25]. Biologically induced mineralisation is a process where bacteria produce biominerals, commonly as a secondary event from interactions between the activity of the microorganisms and their surrounding environments [26]. The formation of phosphate minerals has frequently been observed in sedimentary environments where biological productivity is high [27]. Since *G. sulfurreducens* is a ubiquitous species in sediments and soils, it can have a relevant effect on corrosion and the corrosion protection of buried industrial equipment such as off-shore and harbour structures, oil and gas pipes and buried storage tanks [28]. Nevertheless, this bacterial genus has mainly been studied in the context of microbial fuel cells rather than that of corrosion.

Although *Geobacter metallireducens* and *Shewanella oneidensis* have been equally studied concerning their role in biomineralisation and their use of Fe (III) as terminal electron acceptor in anaerobic respiration processes, only *Shewanella* has been studied in relation to corrosion processes [19,29,30].

Corrosion studies involving iron reducing bacteria such as *G. sulfurreducens* have been reported only by Mehanna et al. [3,13,28]. Other studies have dealt with the behaviour and characteristics of these bacteria, such as their electroactivity, their environmental role concerning iron sources and bio-mineralisation, and their metabolism [22–24,31,32]. Moreover, little work has been done to examine which iron reducing microbial species are prevalent within bacterial communities that lead to corrosion [20]. Considering the lack of knowledge about the influence of these bacteria in corrosion, the objective of the present study is to find out whether *G. sulfurreducens* is able to protect carbon steel against corrosion and, if so, what the mechanism of inhibition is.

In the present work, the concentrations of electron donor (acetate) and electron acceptor (fumarate) were considerably reduced for the electrochemical experiments with the aim of diminishing the likelihood of biofilm formation through the scarcity of carbon source. Thus the interference of EPS and of the complex biofilm itself in the electrochemical behaviour was reduced. Furthermore, lowering the acetate concentration would unbalance the redox state of the bacterial cells, forcing them to search for a new source of electrons on the material surface. All these altered conditions (electron acceptor and donor and phosphate concentration) would make it possible to see the response of the bacteria on carbon steel in conditions much closer to those of the environments where this type of bacteria may live. The final objective was to determine whether *G. sulfurreducens* enhances or inhibits the corrosion of carbon steel in these conditions.

2. Experimental procedure

2.1. Bacteria and media

The *G. sulfurreducens* ATCC 51573 strain used for the experiments was obtained from DSMZ (Deutsche Sammlung von Mikroorganismen und Zellkulturen). The media and solutions were prepared following the DSMZ protocol [33]. The culture growth medium contained 28 mM NH_4Cl, 5 mM NaH_2PO_4, 1.3 mM KCl, 29.7 mM $NaHCO_3$ and 10 mM sodium acetate (electron donor). The medium was sterilised by autoclaving at 121 °C for 15 min. Once the medium had cooled down, a sodium fumarate solution (electron acceptor) filtered with a 0.2 μm pore filter was added to obtain a final concentration of 50 mM of fumarate in the medium. 10 mL/L of vitamins (ATCC MD-VS) and 10 mL/L of minerals solution (ATCC MD-TMS) were also added.

The *G. sulfurreducens* culture was performed in anaerobic glass vials with 50 mL of growth medium. The vials were sealed with butyl rubber septa and de-aerated by injecting N_2/CO_2 (80:20, v/v) at least 30 min before the injection of bacteria (10% of bacterial initial suspension). This first incubation lasted for 3–5 days at 30 °C for optimum bacterial growth. The culture was ready for inocula-

Please cite this article in press as: C. Cote et al., *Geobacter sulfurreducens*: An iron reducing bacterium that can protect carbon steel against corrosion?, Corros. Sci. (2015), http://dx.doi.org/10.1016/j.corsci.2015.01.044

tion into the electrochemical reactors once the absorbance in the anaerobic vials reached around 0.3. The number of planktonic cells was evaluated by measuring the absorbance at 620 nm. The absorbance was related to the number of cells expressed in Colony Forming Units per millilitre (CFU mL^{-1}) by the following calibration formula [34]:

$$[\text{CFU mL}^{-1}] = \text{OD}_{620\text{nm}} \times 472,067 \quad (1)$$

where OD is the optical density measured at 620 nm.

The anaerobic reactors used for the electrochemical measurements were filled with medium containing all the chemical compounds found in the growth medium, most of which were at the same concentrations. Only the electron donor and acceptor concentrations were adjusted: to 1 mM acetate and 10 or 25 mM fumarate.

2.2. Electrochemical measurements

Anaerobic reactors of 0.5 L were used for experiments with *G. sulfurreducens,* the liquid level being adjusted to give a total volume of 300 mL. The anaerobic conditions were obtained by bubbling N_2/CO_2 80:20 into the reactors for at least 45 min before inserting the metal coupons. The flow of N_2/CO_2 was maintained during the whole experiment unless stated otherwise. Reactors were kept in a thermal bath in order to ensure a constant temperature (30 °C) during experiments; pH was measured for all the experiments at the initial time ($h = 0$) and final time ($h \geqslant 144$ h).

The working electrodes (WEs) were 2-cm-diameter cylinders of AISI C1145 carbon steel. The nominal chemical composition for the steel C1145 is shown in Table 1.

The WE was covered by a polymeric coating (thermo-contractible polyolefin, ATUM®) leaving a flat disk of the surface uncovered, with a total exposed area of 3.14 cm^2. Connections were made through titanium wire protected with the same polymeric coating. The electrodes were ground using SiC paper with P120–P600 grit until a smooth surface was achieved. Grinding was followed by cleaning with ethanol (70%) and thorough rinsing with sterile distilled water.

For all the experiments, electrochemical measurements were performed using a multipotentiostat (VMP-Bio-Logic) with a platinum grid (Pt, Ir 10%) used as counter electrode (CE). A silver wire coated with silver chloride (Ag/AgCl) was used as the reference electrode (RE). Since the chloride concentration of the electrolyte was 0.03 M, the potential of the reference was $E = 0.223 - 0.059 \log[Cl^-] = 0.31$V vs. SHE.

The open circuit potential, OCP, was measured over time for all the experiments. Electrochemical Impedance Spectroscopy (EIS) was used to obtain information on the interface, using a frequency from 100 kHz to 10 mHz and an amplitude of 10 mV. The techniques described above were combined in order to obtain information on the electrochemical system formed by the metal coupon in the electrolyte and the influence of the electroactive bacteria *G. sulfurreducens* on the system. The combination of these 2 techniques together with surface analysis constitutes a good tool for studying corrosion and electrochemical systems.

The carbon steel coupons were immersed in the de-aerated reactor medium containing 5 mM of NaH_2PO_4, 1 mM acetate as electron donor and 10 mM or 25 mM fumarate as electron acceptor. The concentrations of electron donor and electron acceptor were considerably lower in the electrochemical experiments than in the growth medium in the aim of reducing biofilm formation, which could interfere with the electrochemical behaviour. Likewise, lowering the acetate concentration would favour the electronic exchange between the metal coupon and the bacteria. On the other hand, phosphorus is an essential ingredient for bacterial development and it was added into the medium in the form of sodium phosphate, which was expected to bind with the ferrous ions to form vivianite.

The electrochemical measurements were performed on abiotic control systems and biotic inoculated systems during at least 144 h. The de-aerated conditions were maintained for at least the first 90 h of measurements and, from that time on, as stated in the results, air was allowed to enter the system and restored aerobic conditions. Note that the results given in this paper come from experiments carried out 6 times for the systems with bacteria (1 of them with injection of compressed air) and 5 times for the control system (1 of them with injection of compressed air); reproducibility was found to be high.

Table 1
Chemical composition of AISI C1145 (wt%).

Alloy	Ni	C	Mn	Cu	Si	S	P	Mo	Cr
1145	0.10	0.46	0.65	0.11	0.31	0.03	0.01	0.02	0.10

2.3. Analytical techniques

Total iron in solution was determined by Inductively Coupled Plasma (ICP) analysis using a Horiba ICP–OES ULTIMA2. Twenty mL of the sample was used for total iron measurement and samples were taken 3 times in the first 98 h (the conditions were kept anaerobic during this time). The total iron was not measured in presence of oxygen because oxygen could interfere with the measurements by precipitating soluble iron, which would result in measurements not representing the real total iron dissolved in the medium.

2.4. Surface analysis

Scanning Electron Microscopy (SEM) images were taken using a Hitachi TM3000 Analytical Table Top Microscope at 7000× magnification, working at 15 kV acceleration voltage. The coupons were washed with distilled water and dried with the N_2/CO_2 80:20 gas mixture after 140 h of immersion in the media described.

Energy dispersive X-ray spectroscopy (EDX) was used for elemental analysis of the surface of the coupons.

3. Results and discussion

3.1. Open circuit potential results

Coupons of AISI carbon steel C1145 (composition given in Table 1) were immersed in the electrochemical reactors filled with a medium containing 5 mM of NaH_2PO_4, 1 mM acetate as electron donor and 10 or 25 mM fumarate as electron acceptor, among other compounds. The metallic coupons were set up in the reactors 24 h before inoculation under anaerobic conditions: N_2/CO_2 (80:20) flow was maintained during the first 98 h of the experiment. At time $t = 98$ h, the N_2/CO_2 was stopped and air was allowed to come into the system by opening one of the exits of the reactor in sterile conditions or by injecting sterile compressed air.

At 24 h, the reactors were inoculated with 5% (v/v) of cell culture containing approximately 1.42×10^5 CFU mL^{-1}. In the control reactors, 5% inoculum was also injected but this time filtered on 0.2 μm porous cellulose filter in order to remove the bacterial cells. In this way the chemical composition of all the injected solutions was identical, including the presence of metabolites but no bacterial cells entered the control reactors. The electrochemical behaviour of the system was tested by recording the open circuit potential vs. time. The electrochemical experiments and the main

Please cite this article in press as: C. Cote et al., *Geobacter sulfurreducens*: An iron reducing bacterium that can protect carbon steel against corrosion?, Corros. Sci. (2015), http://dx.doi.org/10.1016/j.corsci.2015.01.044

Table 2
Initial and final OCP for C1145 steel electrodes at the start and the end of the experiments performed in systems with or without bacteria using 1 mM of acetate (electron donor), 10 or 25 mM of fumarate (electron acceptor) and 5 mM of phosphate.

Type of experiment	Fumarate (mM)	Initial OCP (V vs. Ag/AgCl)	Final time *t* (h)	Final OCP (V vs. Ag/AgCl)	*t* (h) in anaerobiosis	OCP jump (V) at t (h)
Control experiments (without bacteria)	25	−0.80	149	−0.55	95	+0.25/100 h
	10	−0.81	143	−0.49	98	+0.32/105 h
	10	−0.82	140	−0.56	90	+0.26/120 h
	10	−0.81	141	−0.28	90	+0.53/95 h
	10	−0.81	135	−0.45	90	+0.36/90 h[a]
Inoculated experiments (with bacteria)	10	−0.80	130	−0.45	70	+0.35/74 h
	10	−0.81	144	−0.79	90	NA[a,b]
	25	−0.78	142	−0.78	95	NA
	10	−0.81	140	−0.79	98	NA
	10	−0.81	168	−0.85	120	NA
	10	−0.81	168	−0.8	120	NA
	10	−0.81	157	−0.79	100	NA

[a] Experiments marked with (a) received injection of air instead of air entrance by opening the reactor.
[b] NA: Not applicable because no OCP jump was observed.

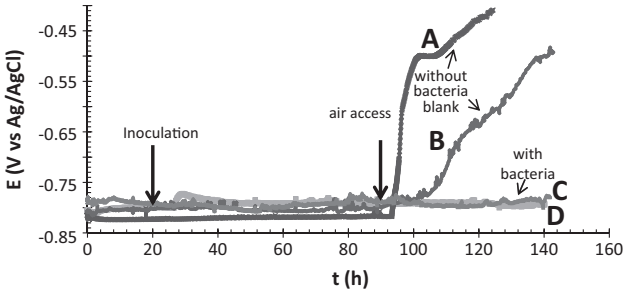

Fig. 1. Variation of OCP over time for electrodes of AISI carbon steel C1145 in medium containing 1 mM sodium acetate (electron donor), 10 mM of sodium fumarate (electron acceptor) and 5 mM phosphate, in presence of 5% *G. sulfurreducens* (C and D) or without bacteria (A and B). A and D: air entrance by air injection; B and C: air entrance by opening the reactors.

results are summed up in Table 2. Fig 1 describes the OCP behaviour of 4 experiments running in parallel: two control systems (curves A and B) and two systems with bacteria (curves C and D). OCP remained stable over time in the 4 reactors under anaerobic conditions.

When air entered the reactors, an OCP jump was observed for the electrodes in the control systems, whereas little or no increase was observed in the systems with bacteria if anaerobic conditions had been maintained for at least 90 h. Note that the results of all the experiments described in Table 2 show high reproducibility regardless of the fumarate concentration.

3.1.1. Anaerobic system (t = 0 to t = 98 h)

Generally, OCP results in anaerobic conditions show that the corrosion potential remained stable (Fig. 1). However, a small increase in the OCP (+15 mV) was observed a few hours after inoculation in the systems where cells were inoculated (Fig. 1, curves C, D).

This small increase of OCP was also found by Mehanna et al. [28] in experiments with *G. sulfurreducens* in a similar medium using the same type of electrode, C1145. They observed a small OCP increase during the first 20 min after inoculation of bacteria, followed by a larger jump of OCP (+300 mV) in the next 3 h. When observing the coupon surfaces, they stated that the presence of bacteria changed the corrosion pattern by grouping corrosion attack into large zones and setting up cathodic electron transfer in places where the cells were growing, which protected the metal against corrosion.

Table 3
ICP results for total dissolved iron. (A) Control system, (B) inoculated system.

t (h)	Fe (mg/L)
A Control/abiotic	
24	5.22 ± 0.3
26	4.68 ± 0.07
92	8.46 ± 0.1
B Inoculated/biotic	
24	5.11 ± 0.25
26	4.37 ± 0.05
92	1.37 ± 0.08

The experiments reported here did not give exactly the same results as obtained by Mehanna et al. [28] although conditions were very similar. The large potential increase in presence of bacteria observed in [28] only 3 h after inoculation and not observed here might be explained by comparing the initial OCP values: the initial potential reported in [28] was around −600 mV vs. Ag/AgCl, which is nearly 200 mV more positive than the one observed here. Having lower potential makes it easier for bacteria to reduce Fe(III) to Fe(II). Fe (II) ions could then bind with phosphate, producing iron phosphate that could protect the metal against a possible increase of OCP.

In conclusion, the small increase in OCP indicated an increase of the cathodic reaction due to the reduction of Fe (III) ions to Fe (II), which led to the formation of an iron (II) phosphate, probably vivianite. This slight increase in potential led to an initial activation of the interface and thus an initial acceleration of the corrosion rate, which decreased after the vivianite formation.

Additionally, total dissolved iron was measured by ICP at 3 different times (at *t* = 24 h, just before inoculation, at *t* = 26 h, after inoculation and at *t* = 92 h, before oxygen was admitted) results show that, at times 24 h and 26 h, a very similar concentration of iron was found in both systems, confirming the reproducibility of the tests (Table 3). The slight decrease of dissolved iron at time 26 h may be explained by precipitation of iron oxide due to the entry of a small amount of oxygen during the inoculation. At time 92 h, an increase in the iron concentration was observed in the control abiotic system whereas there was a decrease in the biotic inoculated one. Moreover, the quantity of total dissolved iron at hour 92 was 6 times lower in the system with bacteria (1.37 mg/L) than in the control system (8.46 mg/L). This can be explained by the precipitation of iron phosphate compound in presence of

Please cite this article in press as: C. Cote et al., *Geobacter sulfurreducens*: An iron reducing bacterium that can protect carbon steel against corrosion?, Corros. Sci. (2015), http://dx.doi.org/10.1016/j.corsci.2015.01.044

Table 4
Comparison of initial and final pH values for systems with a metal coupon C1145 in presence of *G. sulfurreducens* (inoculated experiments) and without bacteria (control systems).

Type of experiment	[fumarate] (mM)	pH initial	pH final
Control experiments (without bacteria)	25	6.9	7.5
	10	6.9	7.5
	10	6.9	7.6
	10	6.8	7.2
	10	6.8	8.4
Inoculated experiments (with bacteria)	10	6.8	7.1
	25	6.8	7.2
	10	6.8	7.4
	10	6.8	7.0
	10	6.8	6.9
	10	6.8	7.0

bacteria since the Fe II, coming from Fe III reduction catalysed by *G. sulfurreducens*, bound with the phosphate, can form either the vivianite layer on the surface of the coupon or phosphate precipitates in the solution.

3.1.2. Aerobic system ($t = 98$ h to $t = 140$ h)

Without stopping OCP measurements, the 4 reactors described above (Fig. 1) were exposed to aerobic conditions at $t = 98$ h. Once the injection of N_2/CO_2 stopped and air was allowed to enter the reactor, either by opening the reactor (curves B, C) or by injecting compressed air (curve A, D), a potential increase of over 300–400 mV was observed in the control reactors (without bacteria, curves A, B) whereas the OCP of the reactors with bacteria remained stable (curves C, D). As was expected, the increase of OCP in the control system was much faster when the compressed air was injected (curve A) than in the experiment where air was allowed to enter the system by the opening of one of the reactor closing capsules (curve B). When the air was injected, the potential increase was observed immediately whereas, when the reactor was opened, the increase in OCP was observed after a delay of 5–20 h.

The OCP or corrosion potential increase observed in the control systems indicates that the system changed drastically, switching the cathodic reaction from water reduction to oxygen reduction, which induced higher corrosion rates [35].

In contrast, the stability of the OCP in the inoculated system indicates that the presence of bacteria prevented the acceleration of the cathodic reaction seen in the control system, due to the coating of iron (II) phosphate that was formed only when bacteria were inoculated. Therefore, *G. sulfurreducens* catalysed the formation of a protective layer against corrosion that was able to prevent the increase of corrosion when oxygen was present in the system, reducing its oxidant action on the metal.

Moreover, an OCP increase was observed when the anaerobic conditions were stopped before 90 h of immersion in the systems with bacteria (Table 2, curve not shown). It can thus be assumed that a minimum of 90 h of anaerobic conditions is needed to create a homogeneous vivianite layer that may protect the surface against corrosion in the presence of oxygen. It is also known that *G. sulfurreducens* tolerates oxygen but does not reduce iron in its presence [24]. Thus the presence of oxygen before the experiment has been running for 90 h inactivates the bacterial metabolism and impedes the formation of a homogeneous iron (II) phosphate layer.

The pH was measured at the beginning and the end of the experiment (Table 4) and it was observed that the pH in systems with bacteria remained stable (around neutrality) even when the N_2/CO_2 injection stopped and oxygen was allowed to enter into the system, whereas the pH in the control systems was less stable and increased slightly in the range of 7.5–8.0. This is in accordance

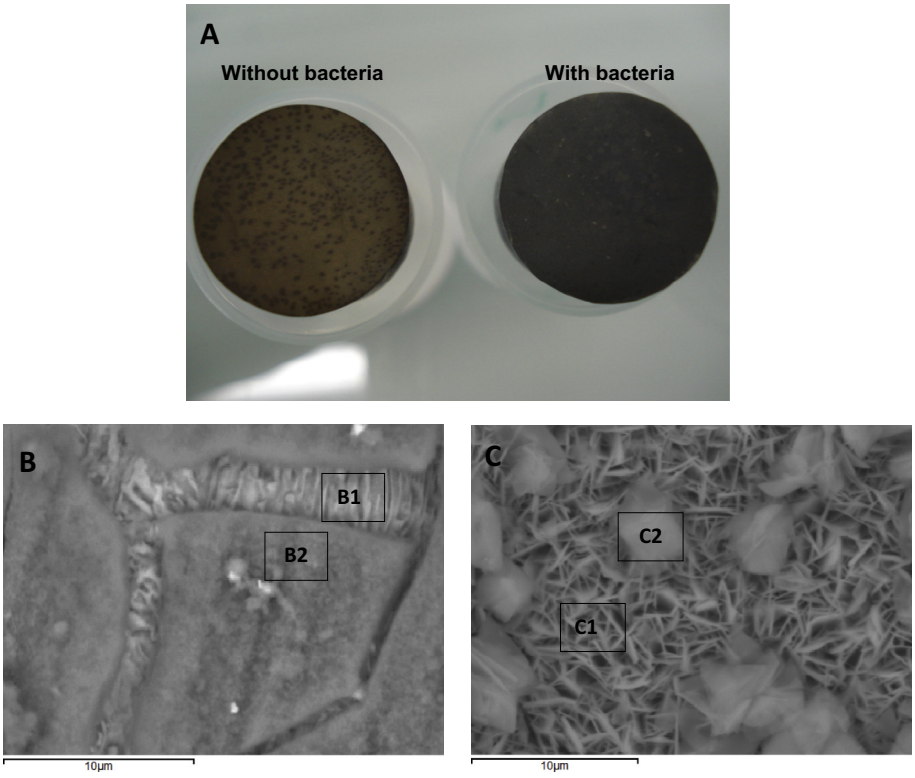

Fig. 2. Macro and micro photographs of coupons after 140 h of immersion: (A) photographs of coupons tested with or without bacteria after oxygen entered the reactors; (B) SEM image of control coupon; and (C) SEM image of coupon tested with bacteria.

Please cite this article in press as: C. Cote et al., *Geobacter sulfurreducens*: An iron reducing bacterium that can protect carbon steel against corrosion?, Corros. Sci. (2015), http://dx.doi.org/10.1016/j.corsci.2015.01.044

Table 5
EDX analysis of coupons surface after 140 h of immersion. (A): clean coupon after grinding (no immersion); B1 and B2: control coupon (see Fig. 2B); C1 and C2 coupon in presence of bacteria (see Fig. 2C).

Element	Weight%	Atomic%
A Clean coupon		
Carbon	4.3	17.3
Iron	95.7	82.7
Control coupon		
B1		
Carbon	15.0	38.3
Oxygen	10.2	19.6
Phosphorus	1.5	1.5
Iron	72.1	39.6
B2		
Carbon	8.4	15.1
Sodium	2.5	2.3
Magnesium	0.6	0.5
Phosphorus	10.5	7.3
Manganese	1.4	0.6
Iron	29.3	11.3
Oxygen	46.3	62.3
Inoculated coupon		
C1		
Carbon	5.5	13.4
Oxygen	21.3	38.9
Sodium	1.4	1.8
Phosphorus	18.6	17.5
Manganese	3.7	1.9
Iron	48.0	25.1
C2		
Carbon	22.2	34.0
Oxygen	45.4	52.1
Sodium	1.1	0.8
Phosphorus	9.9	5.9
Manganese	0.9	0.3
Iron	20.0	6.6

with the oxygen reduction occurring at a higher rate in the absence of bacteria.

3.2. Macro and microscopic results

3.2.1. Macroscopic observations

Macroscopic observations (Fig. 2) performed on the coupons after 140 h of immersion showed that a grey layer had formed on the surface of the coupon when bacteria were present (Fig. 2A, right) whereas, on the coupon without bacteria, there was a yellowish layer that appeared to be an iron oxide usually seen when corrosion takes place in the presence of oxygen [36] (Fig. 2A, left). To approximately determine the conductivity of the deposited layers, a voltmeter was used, touching the surface of the coupon at two points 1 cm apart: an insignificant current was obtained on the grey layer ($r > 6$ MΩ, poorly conductive) whereas some current was detected on the surface of the control coupon ($r < 0.2\Omega$).

3.2.2. Morphology and composition analysis

Microscopy observations showed a needle-like layer distributed homogeneously on the surface of the coupon tested in presence of bacteria (Fig. 2: C1) and some deposits with a random distribution of what it appeared to be a rhombohedral mineral (Fig. 2: C2). In contrast, coupons coming from control experiments exhibited uniform corrosion features with a flat cracked layer (Fig. 2: B2) covering what seemed to be pure iron (Fig. 2: B1).

These observations suggested that the grey layer formed on the coupon in presence of bacteria was iron phosphate (Fig. 2: C1) and that the surface layer of the control coupon was mainly iron oxide.

Surface analysis using energy dispersive X-ray spectroscopy (EDX) (Table 5) confirmed that the layer formed on the surface of the coupon with bacteria was an iron phosphate, most probably vivianite $Fe_3(PO_4)_2{\cdot}8H_2O$ (Table 5: C1) and that the rhombohedral deposit was iron carbonate ($FeCO_3$) (Table 5: C2), commonly known as siderite.

It is also important to point out that the SEM pictures of Fig. 3B and C did not undergo a biofilm fixation procedure and therefore biofilm was not observed. The slight development of bacteria in solution (4.25×10^4 CFU mL^{-1} at 90 h) was sufficient to induce a thin biofilm attached to the surface of the coupon and then the formation of the phosphate layer, vivianite. It was expected that conditions of the medium, which provided a limited carbon source (1 mM of acetate), would force the bacteria to search for a new source of electrons on the material surface. It is presumed that this thin biofilm layer was easily removed by the washing procedure.

3.3. Electrochemical impedance measurements

EIS measurements were performed every 24 h on both the inoculated and control systems. Note that these two experiments ran in parallel for 144 h. The curves at $t = 24$ h correspond to the only measurement performed before inoculation. Curves shown up to time $t = 96$ h are for anaerobic conditions. Afterwards, aerobic conditions were achieved by opening the reactor and allowing air to come into the systems in sterile conditions.

3.3.1. Control system

Fig. 3 shows the impedance response for carbon steel exposed in the control reactor (without bacteria). The Nyquist diagrams (global and zoom, Fig. 3A and B) display the presence of two depressed semi-circles at high (HF) and low (LF) frequencies. The Bode plot and imaginary modulus vs. frequency diagram (Fig. 3C and D) confirm the occurrence of these two time constants. As the two signals belong to two clearly distinct frequency domains, they were analysed separately using the sum of two parallel circuits. The electrolyte resistance R_s and the parameters corresponding to the depressed semi-circles were calculated using an $R_s + Q_1//R_1 + Q_2//R_2$ model (Fig 4) where Q corresponds to a CPE (constant phase element), the impedance of which can be described by (Eq. (2)) [37,38]:

$$Z_{CPE} = 1/Q(\omega)^{\alpha} \times [\cos(\alpha\pi/2) - j\sin(\alpha\pi/2)] \quad (2)$$

where α and Q are the CPE characteristic parameters.

As can be seen in Table 6, the electrolyte resistance varied little throughout the test (values around 40–61 Ω cm^2).

The HF signal was first simulated using the HF part of the circuit shown in Fig. 4 in order to calculate α_1 and R_1 (Table 6 HF oxide). The coefficient α_1 was equal to 0.6, expressing a heterogeneous distribution of the capacitance, and the resistance R_1 (corresponding to the diameter of the semi-circle) was stable since the anaerobic conditions were maintained (around 20 Ω cm^2), and then increased when oxygen was admitted. At the end of the test, R_1 was 8 times higher (at $t = 144$ h) than at the beginning.

However, as the experiment was not performed for frequencies higher than 100 kHz, very few HF points were available and determination of Q was difficult. In order to overcome this shortcoming and to better determine the phenomenon linked to this HF semi-circle, an approximate estimation of the capacitance values was made by means of Eq. (3), using the frequency at the maximum of the circle as would be done for a pure capacitance:

$$C = 1/(2\pi * f_{max} * R) \quad (3)$$

The capacitance values obtained (between 0.16 and 0.33 μF cm^{-2}, Table 6), can be related to an oxide layer (values are too small to be attributed to a double layer even though it

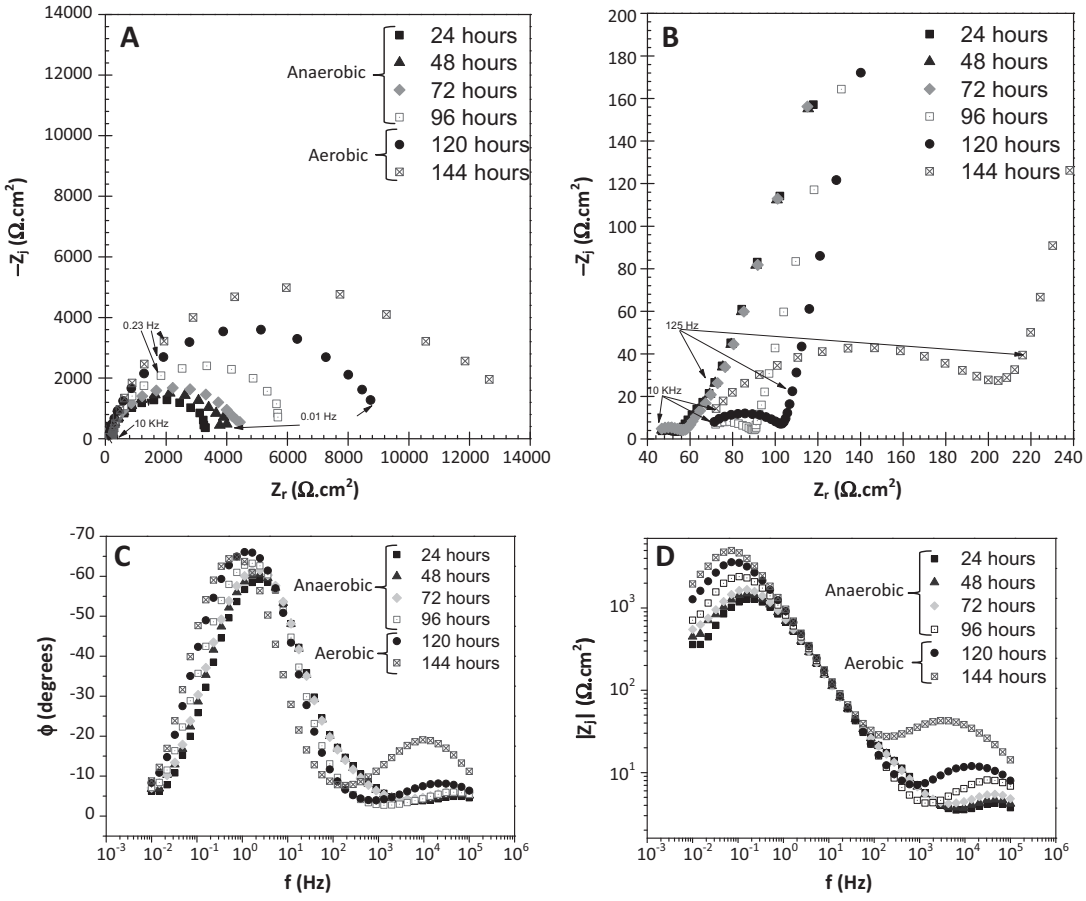

Fig. 3. Impedance diagrams of carbon steel C1145 plotted at OCP during the 144 h of immersion in the control reactor (without bacteria); medium containing 29 mM chloride, 1 mM acetate, 10 mM of fumarate and 5 mM of phosphate. System kept in anaerobic conditions until t = 96 h as indicated in the graphs. (A) Nyquist plot, (B) Nyquist zoom-in, (C) bode phase angle vs. frequency and (D) imaginary modulus vs. frequency.

may be thought that values were under-estimated by the way they were evaluated), the thickness (δ) of which was estimated by Eq. (4).

$$\delta = \varepsilon\varepsilon^{\circ}/C \tag{4}$$

with ε° the vacuum permittivity, equal to 8.85×10^{-14} F cm^{-1}, and ε the permittivity inside the oxide, equal to 12, which is the number habitually used for iron oxides.

The thickness was evaluated to be 50–65 nm and tended to decrease to around 30 nm in the presence of oxygen (Table 6). These values are in the range of those found on this kind of steel (4 nm < δ < 100 nm) [39–41] after immersion in different media in presence or absence of oxygen. The thickness of the oxide films is believed to be affected more by the medium composition (for instance, it decreased under chloride exposure) than the immersion time.

At lower frequency (<1 kHz), linear parts were observed on the plot of the modulus of the imaginary component of the impedance vs. the frequency in logarithmic coordinates (Fig. 3D). The slope values of these linear parts were used for the calculation of alpha (α_2) values in order to determine whether the system had constant phase element (CPE) behaviour or purely capacitive behaviour [37,38,42]. For all instants, the α_2 values found and displayed in Table 6 were lower than 1, confirming a CPE behaviour, i.e. the system exhibited a heterogeneous distribution of time constants. The Q and R values (Table 6) were calculated using the $(R_s + R_1) + Q_2//R_2$ model presented in Fig. 4B considering the LF contribution only.

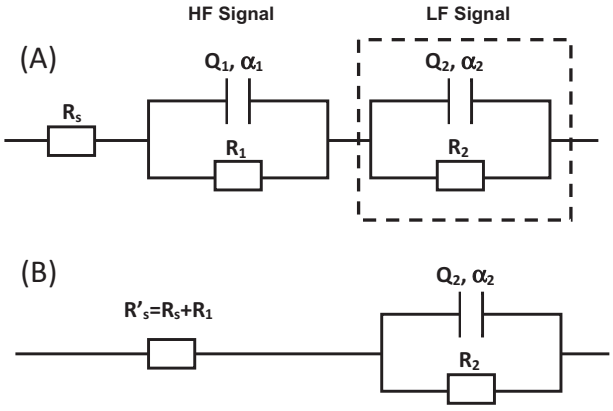

Fig. 4. (A) $R_s + Q_1//R_1 + Q_2/R_2$ model to fit two distinct depressed semi-circles observed on Nyquist plot. R_s = solution resistance, R_1 and R_2 resistances corresponding to the circle diameters at HF and LF respectively, Q_1, α_1 and Q_2, α_2 the characteristic parameters of constant phase elements at HF and LF respectively. (B) $R'_s + Q_2/R_2$ model to fit the depressed semi-circle observed at LF taking only the LF contribution into account. $R'_s = R_s + R_1$.

The effective capacitances associated with the CPE were calculated using Eq. (5), which was derived by Brug et al. [43]:

$$C_{dl} = Q^{1/\alpha}(1/R'_s + 1/R_{ct})^{(\alpha-1)/\alpha} \tag{5}$$

with $R'_s = R_s + R_1$

Table 6
Control system: evolution in time of impedance parameters for a C1145 coupon immersed in a medium containing 1 mM of acetate, 10 mM of fumarate and 5 mM of phosphate in anaerobic (24–96 h) and aerobic (120–144 h) conditions. The EIS parameters correspond to the model presented in Fig. 4 with R_s the solution resistance, R_1 the oxide layer resistance at HF, α_1 the CPE characteristic parameter at HF, C_{ox} the oxide layer capacitance calculated by Eq. (3), δ the thickness of the oxide layer, α_2 and Q_2 the CPE characteristic parameters at LF, R_2 the charge transfer resistance (R_{ct}) and C_{dl}, the double layer capacitance calculated using Brug's Eq. (5).

Time (h)	R_s (Ω cm^2)	HF oxide					LF transfer			
		α_1	R_1 (Ω cm^2)	f_{max} (Hz)	C_{ox} μF cm^{-2}	δ (nm)	α_2	$R_2 = R_{ct}$ (Ω cm^2)	Q_2 (Ω^{-1} cm^{-2} s$^{\alpha}$)	C_{dl} μF cm^{-2}
24	41	0.6	17	45,562	0.21	52	0.80	3570	2.6×10^{-04}	83
48	40	0.6	18	45,562	0.19	56	0.80	4113	2.6×10^{-04}	82
72	39	0.6	22	45,562	0.16	68	0.81	4527	2.5×10^{-04}	84
96	61	0.6	33	30,739	0.16	67	0.84	6139	2.1×10^{-04}	90
120	61	0.6	50	14,013	0.23	46	0.85	9263	1.9×10^{-04}	86
144	59	0.6	166	2905	0.33	32	0.87	12,246	1.8×10^{-04}	88

The values of capacitances varied from 82 to 90 μF cm^{-2}. These values correspond to double layer capacitance values. Thus it can be assumed that the CPE behaviour was due to the surface distribution of time constants linked to the charge transfer. Consequently, the diameter of the depressed semi-circles can be attributed to a charge transfer resistance, R_{ct} that increases as the duration of immersion increases. As a first approach, it can be assumed that this increase indicates a decrease in the corrosion rate since the electron transfer on the interface decreases. However, the R_{ct} increase is greater in the presence of oxygen (from 6 to 12 kΩ cm^2 in 40 h) than in anaerobic conditions (from 4 to 6 kΩ cm^2 in 96 h).

Combining the analysis of these results with those of OCP and surface analysis, it seems that a layer of magnetite is formed first, as normally happens in abiotic anaerobic conditions [44–46]. This layer increasingly protects the material (increase of R_{ct}) but not enough to avoid the action of oxygen: by modifying the redox potential (strong oxidising agent), the input of oxygen may promote the formation of a new oxide layer due to a change in the oxidation state of the iron, probably from iron (II) oxides to iron (III) oxides. This growing oxide layer protects the surface against corrosion (R_{ct} doubles in 40 h). However, it must be keep in mind that an oxide layer on carbon steel is not very strong and not very protective against further corrosion, mainly because of its porosity.

3.3.2. Inoculated system

In biotic conditions (5% of bacterial inoculum), on the Nyquist plots (Fig. 5A and B), two depressed semi-circles could also be observed as in abiotic conditions. Their diameter increased as the duration of immersion increased. The EIS results were analysed as for the control system and the values calculated for the different parameters are grouped together in Table 7.

At HF (HF oxide), when bacteria were inoculated, C_{ox} decreased (values between 0.061 and 0.071 μF cm^{-2}, smaller than in an abiotic medium) and remained stable as long as the conditions remained anaerobic. These results show that the HF signals can be attributed to an iron oxide layer that is certainly more reduced than the one found in the control system, due to the presence of bacteria, and certainly contains phosphate species. Then, after oxygen entered the system, Cox decreased again to reach a stable value (around 0.030 μF cm^{-2}). In terms of layer thickness (estimated to a first approximation using Eq. (4) and taking $\varepsilon = 12$), δ increased after inoculation in anaerobic conditions and then was maintained at around 300 nm thick in the presence of oxygen. The resistance linked to this layer also increased gradually from 23 to 53 Ω cm^2.

At LF, a linear part was found on the modulus diagram of the impedance where the imaginary component was plotted against the frequency (Fig 5D) for each immersion time. The corresponding slopes had values lower than 1, confirming CPE behaviour. The R_2 and Q_2 were calculated using the $R'_s + Q_2//R_2$ model presented in Fig. 4B considering only the LF contribution (LF circuit circled in black dashed lines) and the effective capacitances associated with Q using Brug's Eq. (5) (Table 7). The capacitance values were in the range of 59–93 μF cm^{-2} and could thus be attributed to a double layer capacitance (C_{dl}). Consequently, R_2 values corresponded to values of a charge transfer resistance. When the immersion time increased, R_{ct} increased – more sharply after the entrance of oxygen: R_{ct} (22 kΩ cm^2 at $t = 144$ h) was 3 times higher than the R_{ct} value observed at the end of the anaerobic period ($t = 96$ h). In other words, at the end of the experiment, the interface was such that the charge transfers slowed down over time. Since the presence of oxygen has no impact on OCP value, it can be assumed that the iron phosphate layer (probably vivianite) that grew in the anaerobic conditions due to the presence of *G. sulfurreducens* protected the surface against further corrosion even in aerobic conditions.

3.3.3. Comparisons of the two systems (abiotic and inoculated)

When comparing the control system and the system with bacteria, it was observed that, although there were similarities in the plots obtained up to hour 96 (i.e. in anaerobic conditions), differences were observed once oxygen (air) entered the reactor. The system with bacteria showed a higher R_{ct}, which could be related to a lower corrosion rate due to the presence of bacteria. The stability of the OCP and the surface analysis, combined with EIS results confirmed that the Iron (II) phosphate layer (vivianite) formed on the coupon surface of inoculated systems was less conductive and more protective than the oxide layer formed in the control system. Thus, it is a protective type of coating without being a passive layer. In contrast, the iron (II, III) oxide layer (magnetite) found in abiotic systems varied depending on the oxygen presence and, although the charge transfer resistances were increased after a long period of immersion, the oxide layer was not so stable and protective as the vivianite layer.

In the present work, the formation of vivianite by *G. sulfurreducens* using a carbon steel coupon as the electron acceptor is reported for the first time. Based on the electrochemical and surface analysis results, a hypothesis can be proposed for the mechanism of inhibitive layer formation by *G. sulfurreducens*. Initially, when no oxide layers are present, dissolution of iron takes place at a low rate due to the absence of oxygen and finally forms an iron oxide layer of magnetite, $FeO{\cdot}Fe_2O_3$ during the first 24 h of immersion. An IRB such as *Geobacter* may switch from using an organic compound such as fumarate as the sole electron acceptor to a more efficient source of electron acceptor such as Fe(III), to increase the limited amount of ATP [20,47,48]. Thus, once *G. sulfurreducens* is inoculated, it starts interacting with the iron oxide to reduce Fe (III) to Fe (II) as follows:

$$FeO \cdot Fe_2O_3 + 3HPO_4^{2-} + 8H^+ + 2e^- \overset{\text{bacteria}}{\rightarrow} 3Fe(HPO_4) + 4H_2O \quad (6)$$

$$3Fe(HPO_4) \rightarrow Fe_3(PO_4)_2 + HPO_4^{2-} + 2H^+ \quad (7)$$

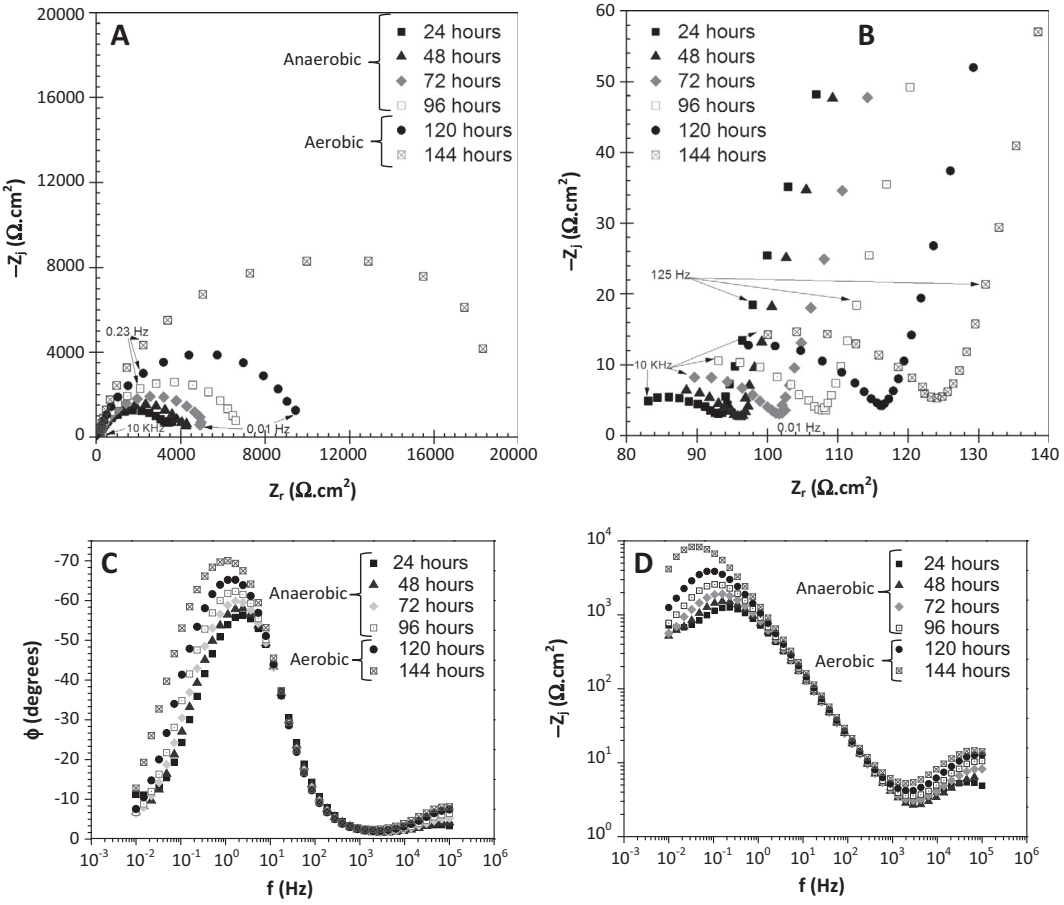

Fig. 5. Impedance diagrams of carbon steel C1145 plotted at OCP during the 144 h of immersion in reactor with *G. sulfurreducens* inoculated at $t = 24$ h with medium containing 29 mM chloride, 1 mM acetate, 10 mM of fumarate and 5 mM of phosphate. Systems were kept in anaerobic conditions until $t = 96$ h as indicated on the graphs. (A) Nyquist plots, (B) Nyquist zoom-in, (C) bode phase angle and (D) imaginary modulus vs. frequency plots.

Table 7
Biotic system: evolution in time of impedance parameters for a C1145 coupon immersed in a medium containing 1 mM of acetate, 10 mM of fumarate, 5 mM of phosphate and inoculated by *Geobacter sulfurreducens* in anaerobic (24–96 h) and aerobic (120–144 h) conditions. The EIS parameters correspond to the model presented in Fig. 4 with R_s the solution resistance, R_1 the oxide layer resistance at HF, α_1 the CPE characteristic parameter at HF, C_{ox} the oxide layer capacitance calculated by Eq. (3), δ the thickness of the oxide layer, α_2 and Q_2 the CPE characteristic parameters at LF, R_2 the charge transfer resistance (R_{ct}) and C_{dl}, the double layer capacitance calculated using Brug's Eq. (5).

Time (h)	R_s (Ω cm^2)	HF oxide					LF transfer			
		α_1	R_1 (Ω cm^2)	f_{max} (Hz)	C_{ox} μF cm^{-2}	δ (nm)	α_2	$R_2 = R_{ct}$ (Ω cm^2)	Q_2 (Ω^{-1} cm^{-2} s$^{\alpha}$)	C_{dl} μF cm^{-2}
24	74	0.6	23	45,562	0.15	69	0.80	3542	2.3×10^{-04}	83
48	72	0.6	26	100,000	0.061	170	0.81	4238	2.2×10^{-04}	83
72	71	0.6	33	67,500	0.071	150	0.83	5140	2.2×10^{-04}	93
96	66	0.6	44	132,500	0.027	390	0.84	6770	2.1×10^{-04}	91
120	73	0.7	46	100,000	0.035	300	0.85	9860	1.8×10^{-04}	89
144	75	0.6	53	67,500	0.045	240	0.84	21,917	1.4×10^{-04}	59

The formation of insoluble iron phosphate depends on the metal ions present in solution close to the interface, the concentration of phosphate ions in the solution, and the reactivity of metal surface.

4. Conclusions

The presence of *G. sulfurreducens* in phosphate medium induces the formation of a compact layer of iron (II) phosphate on the surface of carbon steel C1145 immersed in a medium containing 1 mM of acetate, 10 mM of fumarate and 5 mM of phosphate. SEM and EDX analysis showed the formation of this iron (II) phosphate layer (allegedly vivianite) in the system where bacteria were inoculated whereas, in the control system, there was an iron oxide all over the coupon. The formation of the phosphate layer is ensured only when the starting potential of the system is in the range of 750–800 mV vs. Ag/AgCl. This layer maintains the stability of the open circuit potential even after air is allowed to enter the system. It thus prevents an acceleration of the cathodic reaction rate and so an acceleration of corrosion. In contrast, the iron phosphate layer was not formed in the control systems in absence of bacteria, which allowed an increase of the open circuit potential to 400–450 mV once oxygen entered.

EIS showed similarities in the behaviour of systems with and without bacteria. However, observations led to the conclusion that the iron (II) phosphate layer formed in presence of bacteria was somewhat more protective than the iron oxide formed in abiotic

Please cite this article in press as: C. Cote et al., *Geobacter sulfurreducens*: An iron reducing bacterium that can protect carbon steel against corrosion?, Corros. Sci. (2015), http://dx.doi.org/10.1016/j.corsci.2015.01.044

conditions, without being a passive layer. ICP analysis for total iron proved that, in the absence of bacteria, the quantity of iron dissolved in the medium was twice the amount of iron when bacteria were present.

Iron (II) phosphate layers such as vivianite $Fe_3(PO_4)_2{\cdot}8H_2O$ are known to protect metals by forming a barrier between the surface and the surroundings. The layer could have been formed due to an acceleration of Fe (III) reduction to Fe (II) in the presence of microorganisms, which, in contact with the phosphate in the medium, leads to the formation of a vivianite deposit.

In conclusion, *G. sulfurreducens* indeed protected AISI carbon steel C1145 against corrosion in the conditions described, thanks to the formation of an iron (II) phosphate layer that protected the metal against the oxidising action of oxygen.

Acknowledgements

The research leading to these results has received funding from the European Community's Seventh Framework Programme (FP7/2007-2013) under grant agreement n° 238579. Project website: www.biocor.eu/ip2.

The authors would like to thank Dr. Alain Bergel of the Laboratoire de Génie Chimique in Toulouse for helpful discussions about this paper.

References

[1] I. Beech, C.C. Gaylarde, Recent advances in the study of biocorrosion: an overview, Rev. Microbiol. 30 (1999) 177–190. ISSN 0001-3714.
[2] S. Chongdar, G. Gunasekaran, P. Kummar, Corrosion inhibition of mild steel by aerobic biofilm, Electrochem. Acta 50 (2005) 4655–4665.
[3] M. Mehanna, R. Basseguy, M.-L. Delia, A. Bergel, *Geobacter sulfurreducens* can protect 304L stainless steel against pitting in conditions of low electron acceptor concentrations, Electrochem. Commun. 12 (2010) 724–728.
[4] H.-P. Volkland, H. Harms, B. Müller, G. Repphun, O. Wanner, A.J.B. Zehnder, Bacterial phosphating of mild (unalloyed) steel, Appl. Environ. Microbiol. 66 (2000) 4389–4395.
[5] H.-P. Volkland, H. Harms, A.J.B. Zehnder, Corrosion protection by anaerobiosis, Water Sci. Technol. 44 (2001) 103–106.
[6] Y. Gourbeyre, E. Guilminot, F. Dalard, Study of the corrosion layer on iron obtained in solutions of water–polyethilene glycol (PEG400)-sodium phosphate, J. Mater. Sci. 38 (2003) 1307–1313.
[7] R. Zuo, Biofilms: strategies for metal corrosion inhibition employing microorganisms, Appl. Environ. Microbiol. 76 (2007) 1245–1253.
[8] H. Videla, L.K. Herrera, Understanding microbial inhibition of corrosion. A comprehensive overview, Int. Biodeterior. Biodegrad. 63 (2009) 869–900.
[9] F. Mansfeld, The interaction of bacteria in metal surfaces, Electrochem. Acta 52 (2007) 7670–7680.
[10] F. Mansfeld, H. Hsu, D. Ornek, T.K. Wood, Corrosion control using regenerative biofilms on aluminium 2024 brass in different media, J. Electrochem. Soc. 149 (2002) B130–B138.
[11] H. Videla, Manual of Biocorrosion, first ed., CRC-Press, USA, 1997.
[12] S. Da Silva, R. Basseguy, A. Bergel, Hydrogenase-catalysed deposition of vivianite on mild steel, Electrochem. Acta 49 (2004) 2097–2103.
[13] M. Mehanna, R. Basseguy, M.-L. Delia, L. Girbal, M. Demuez, A. Bergel, New hypothesis for hydrogenase implication in the corrosion of mild steel, Electrochem. Acta 54 (2008) 140–147.
[14] J. Duan, S. Wu, X. Zhang, G. Huang, M. Du, B. Hou, Corrosion of carbon steel influenced by anaerobic biofilm in natural seawater, Electrochem. Acta 54 (2008) 22–28.
[15] M. Dubiel, C.H. Hsu, C.C. Chien, F. Mansfeld, D.K. Newman, Microbial iron respiration can protect steel from corrosion, Appl. Environ. Microbiol. 68 (2002) 1440–1445.
[16] B.J. Little, J.S. Lee, R.I. Ray, The influence of marine biofilms on corrosion: a concise review, Electrochem. Acta 54 (2008) 2–7.
[17] M. Eashwar, S. Maruthamuthu, S. Sathiyanarayanan, S. Balarkrishnan, The ennoblement of stainless alloys by marine biofilms – the neutral pH and passivity enhancement model, Corros. Sci. 37 (1995) 1169–1176.
[18] J.B. Little, R. Ray, A perspective of corrosion inhibition by biofilms, Corrosion 58 (2002) 424–428.
[19] L. Esnault, M. Jullien, C. Mustin, O. Bildstain, M. Libert, Metallic corrosion processer reactivation sustained by iron-reducing bacteria: implication on long-term stability of protective layers, Phys. Chem. Earth 36 (2011) 1624–1629.
[20] L.K. Herrera, H. Videla, Role of iron-reducing bacteria in corrosion and protection of carbon steel, Int. Biodeterior. Biodegrad. 63 (2009) 891–895.
[21] H.-P. Volkland, H. Harms, K. Kauffman, O. Wanner, A.J.B. Zehnder, Repair of damaged vivianite coatings on mild steel using bacteria, Corros. Sci. 43 (2001) 2135–2146.
[22] F.S. Islam, R.L. Pederick, A.G. Gault, L.K. Adams, D.A. Polya, J.M. Charnock, J.R. Lloyd, Interactions between the Fe (III)-reducing bacterium *Geobacter sulfurreducens* and arsenate, and capture of the metalloid by biogenic Fe(II), Appl. Environ. Microbiol. 71 (2005) 8642–8648.
[23] D.R. Lovley, E.J.P. Phillips, Novel mode of microbial energy metabolism: organic carbon oxidation coupled to dissimilatory reduction of iron or manganese, Appl. Environ. Microbiol. 54 (1988) 1472–1480.
[24] D. Bond, D.R. Lovley, Electricity production by *Geobacter sulfurreducens* attached to electrodes, Appl. Environ. Microbiol. 69 (2003) 1548–1555.
[25] B. Little, P. Wagner, K. Hart, R. Ray, D. Lavoie, K. Nealson, C. Aguilar, The role of metal-reducing bacteria in microbiologically influenced corrosion, Corr. Paper no. 215. NACE International, Houston, TX, 2000, ISBN: 97215 1997 CP.
[26] R.B. Frenkel, D.A. Bazylinski, Biologically induced mineralization by bacteria, in: P.M. Dove, J.J. De Yoreo, S. Weiner (Eds.), Biomineralization (Reviews in Mineralogy), vol. 54, Mineralogical Society of America, Washington, D.C., 2003, pp. 95–114.
[27] K. Konhauser, Bacterial iron biomineralisation in nature, FEMS Microbiol. Rev. 20 (1997) 315–326.
[28] M. Mehanna, R. Basseguy, M.-L. Delia, A. Bergel, Effect of *Geobacter sulfurreducens* on the microbial corrosion of mild steel, ferritic and austenitic stainless steels, Corros. Sci. 51 (2009) 2596–2604.
[29] M. Libert, O. Bildstein, L. Esnault, M. Jullien, R. Sellier, Molecular hydrogen: an abundant energy source for bacterial activity in nuclear waste repositories, Phys. Chem. Earth. 36 (2011) 1616–1623.
[30] D.P. Lies, M.E. Hernandez, A. Kappler, R.E. Mielke, J.A. Gralnick, D.K. Newman, *Shewenella oneidensis* MR-1 uses overlapping pathways for iron reduction at a distance and by direct contact under conditions relevant for biofilms, Appl. Environ. Microbiol. 71 (2005) 4414–4426.
[31] D.R. Lovley, Magnetite formation during microbial dissimilatory iron reduction, in: R.B. Frankel, R.P. Blakemore (Eds.), Iron Biominerals, Plenum, New York, 1991, pp. 51–166.
[32] D. Lovley, Dissimilatory Fe (III) and Mn (IV) reducing prokaryotes, in: M. Dworkin, S. Falkow, E. Rosenberg, K-H. Shleifer, E. Stackebrandt (Eds.), The Prokaryotes, a Handbook on the Biology of Bacteria, Springer, N.Y., USA, 2006, pp. 635–658. 2.
[33] Deutsche Sammlung von Mikroorganismen und Zellkulturen DSMZ GmbH, Microorganisms, 826. Geobacter medium, 2007.
[34] C. Dumas, R. Basseguy, A. Bergel, Microbial electrocatalysis with *Geobacter sulfurreducens* biofilms on stainless steel cathodes, Electrochem. Acta 53 (2008) 2494–2500.
[35] A.J. Bard, L.R. Faulkner, Electrochemical methods: fundamentals and applications, second ed., in: Introduction and Overview of Electrode Processes, John Wiley and Sons, Inc., 2001. Chapter 1.
[36] D. Jones, Principles and Prevention of Corrosion, second ed., Prentice Hall, New York, 1995.
[37] M.E. Orazem, N. Pébère, B. Tribollet, Enhanced graphical representation of electrochemical impedance data, J. Electrochem. Soc. 153 (2006) B129–B136.
[38] M.E. Orazem, B. Tribollet, Electrochemical Impedance Spectroscopy, John Wiley & Sons publications, NJ, USA, 2008.
[39] P. Ghods, O.B. Isgor, J.R. Brown, F. Bensebaa, XPS depth profiling study on the passive oxide film of carbon steel in saturated calcium hydroxide solution and the effect of chloride on the film properties, Appl. Surf. Sci. 257 (10) (2011) 4669–4677.
[40] O. Girčienė, R. Ramanauskas, L. Gudavičiūtė, A. Martušienė, Inhibition effect of sodium nitrite and silicate on carbon steel corrosion in chloride-contaminated alkaline solutions, Corrosion 67 (2011) 125001-1–125001-12.
[41] M.F. Montemor, A.M.P. Simoes, M.G.S. Ferreira, Analytical characterization of the passive film formed on steel in solutions simulating the concrete interstitial electrolyte, Corrosion 54 (5) (1998) 347–354.
[42] C.S. Hsu, F. Mansfeld, Concerning the conversion of the constant phase element parameter Yo into a capacitance, Corrosion 57 (2001) 747.
[43] G.J. Brug, A.L.G. van den Eeden, M. Sluyters-Rehbach, J.H. Sluyters, The analysis of electrode impedances complicated by the presence of a constant phase element, J. Electroanal. Chem. 176 (1984) 275295.
[44] O. Benali, M. Abdelmoula, P. Refait, J-M.R. Genin, Effect of orthophosphate on the oxidation products of Fe(II)–Fe(III) hydroxycarbonate: the transformation of green rust to ferrihydrite, Geochim. Cosmochim. Acta 65 (2001) 1715–1726.
[45] A. Matthews, Magnetite formation by the reduction of hematite with iron under hydrothermal conditions, Am. Mineral. 61 (1976) 927–932.
[46] T. Iwasaki, N. Sato, H. Nakamura, S. Watano, An experimental investigation of aqueous-phase synthesis of magnetite nanoparticles via mechanochemical reduction of goethite, Adv. Powder Technol. 24 (2013) 482–486.
[47] R. Javaherdashti, Microbially Influenced Corrosion – An Engineering Insight, Springer, London, 2008.
[48] D.R. Loveley, Microbial Fe(III)-reduction in subsurface environments, FEMS Microbiol. Rev. 20 (1997) 305–313.